Climatology and Interannual Variability of Arctic Cyclone Activity: 1948–2002

XIANGDONG ZHANG AND JOHN E. WALSH

International Arctic Research Center, University of Alaska, Fairbanks, Fairbanks, Alaska

JING ZHANG

Geophysical Institute, University of Alaska, Fairbanks, Fairbanks, Alaska

UMA S. BHATT

International Arctic Research Center, University of Alaska, Fairbanks, Fairbanks, Alaska

MOTO IKEDA

Graduate School of Environmental Earth Science, Hokkaido University, Sapporo, Japan

(Manuscript received 27 June 2003, in final form 16 January 2004)

ABSTRACT

Arctic cyclone activity is investigated in the context of climate change and variability by using a modified automated cyclone identification and tracking algorithm, which differs from previously used algorithms by single counting each cyclone. The investigation extends earlier studies by lengthening the time period to 55 yr (1948–2002) with a 6-hourly time resolution, by documenting the seasonality and the dominant temporal modes of variability of cyclone activity, and by diagnosing regional activity as quantified by the cyclone activity index (CAI). The CAI integrates information on cyclone intensity, frequency, and duration into a comprehensive index of cyclone activity. Arctic cyclone activity has increased during the second half of the twentieth century, while midlatitude activity generally decreased from 1960 to the early 1990s, in agreement with previous studies. New findings include the following. 1) The number and intensity of cyclones entering the Arctic from the midlatitudes has increased, suggesting a shift of storm tracks into the Arctic, particularly in summer. 2) Positive tendencies of midlatitude cyclone activity before and after the 1960–93 period of decreasing activity correlate most strongly with variations of cyclone activity in the North Atlantic and Eurasian sectors. 3) Synchronized phase and amplitude variations in cyclone activity over the Arctic Ocean (70°–90°N) and the Arctic marginal zone (60°–70°N) play a critical role in determining the variations of cyclone activity in the Arctic as a whole. 4) Arctic cyclone activity displays significant low-frequency variability, with a negative phase in the 1960s and a positive phase in the 1990s, upon which 7.8- and 4.1-yr oscillations are superimposed. The 7.8-yr signal generally corresponds to the alternation of the cyclonic and anticyclonic regimes of the Arctic sea ice and ocean motions.

1. Introduction

Cyclone activity in the Arctic is a fundamental consideration in studies of high-latitude weather and climate. The wind and precipitation produced by these storms are responsible for some of the most significant impacts of weather in high-latitude communities. Coastal erosion caused by Arctic cyclones is an increasingly serious problem during periods when nearshore waters are free of sea ice. Cyclones also represent a primary mechanism for the transport of heat and moisture into the Arctic, thereby offsetting the deficits that arise from radiative and freshwater imbalances, respectively. In the context of climate and climate change, the likelihood that greenhouse warming will be amplified in the polar regions has interesting implications for Arctic cyclones, since a reduced pole-to-equator temperature gradient may alter the major storm tracks of cyclones affecting the Arctic. However, Boer's (1995) finding that the poleward heat and moisture transports do not necessarily decrease in a greenhouse warming scenario points to the complexity inherent in the relationships between latitudinal temperature gradients, poleward energy fluxes, and cyclone activity. The fact that the Arctic has indeed warmed and sea ice has retreated by 10%–15% in recent decades (Houghton et al. 2001) points to the need for a comprehensive examination of cyclone activity in the Arctic during the latter part of the twentieth century and a better understanding of its trends and variability.

Corresponding author address: Xiangdong Zhang, International Arctic Research Center, University of Alaska, Fairbanks, Fairbanks, AK 99775.
E-mail: xdz@iarc.uaf.edu

Summaries of cyclones in the northern high latitudes date back to the early compilations of Petterssen (1950), Keegan (1958), and Reed and Kunkel (1960), all of whom were constrained by limited data availability. Nevertheless, these early studies indicated that the North Atlantic serves as the primary cyclone conduit between midlatitudes and the Arctic during winter, although some Pacific cyclones were found by Petterssen to impinge on the Arctic periphery during winter. More extensive evaluations of Arctic cyclone activity, based on gridded fields of sea level pressure (SLP), have been provided during the past decade by Serreze et al. (1993), Serreze (1995), and McCabe et al. (2001). The results of Serreze et al. (1993, cf. their Figs. 3 and 7) show clearly the distinction between the Atlantic-dominated distribution of Arctic winter cyclones and the Arctic-wide distribution characteristic of summer. In the same study, trends of Arctic cyclone frequency for the period 1952–89 were shown to be positive and statistically significant for the winter, spring, and summer; the trend for autumn was also positive but not statistically significant. The positive trend for winter was supported by McCabe et al.'s (2001) results for the 1959–97 period, which showed a substantial increase of wintertime cyclones around 1989 [the final year of Serreze et al.'s (1993) study period], which was also the time of a well-documented increase of the Arctic Oscillation (AO) index (Thompson and Wallace 1998). A key question that arises in connection with the AO is whether trends of Arctic cyclone activity are manifestations of their associations with atmospheric modes in which low-frequency variability is prominent. Accordingly, the temporal scales of Arctic cyclone variability will serve as a primary focus of the present study.

In this paper, we extend the earlier studies of Arctic cyclones by 1) documenting the low-frequency variations in each season of a longer time period (1948–2002) than has previously been examined in studies of Arctic cyclones, 2) evaluating the seasonality and trends in the regions of origin of Arctic cyclones, and 3) combining frequency and intensity into a broader assessment of Arctic cyclone variability, particularly as it relates to large-scale atmospheric modes such as the AO.

2. Data, definitions, and methodology

a. Data and study area

This study uses the 6-hourly SLP from the National Centers for Environmental Prediction–National Center for Atmospheric Research (NCEP–NCAR) reanalysis from January 1948 through December 2002. The reanalysis output has a global horizontal resolution of 2.5° × 2.5° (Kalnay et al. 1996).

We define the Arctic region as poleward of 60°N (Fig. 1), although we use a domain extending equatorward to 30°N because cyclones that reach the Arctic can originate in lower latitudes. While 60°N can be viewed as a somewhat arbitrary boundary, it corresponds broadly with the zero contour of the AO mode, and it concurrently separates the ''polar cap'' from the midlatitudes. In view of different surface characteristics, we further separated the Arctic region into two subregions: the Arctic Ocean from 70° to 90°N and the Arctic marginal zone from 60° to 70°N. The former and latter are dominated by ocean/sea ice and continent, respectively. The Arctic marginal zone is the area through which midlatitude cyclone activity directly influences the Arctic. Though this study focuses on the Arctic region, we are also interested in the relationship of cyclone activities between the Arctic region and the midlatitudes. The midlatitudes are defined here as 40°–60°N (Fig. 1).

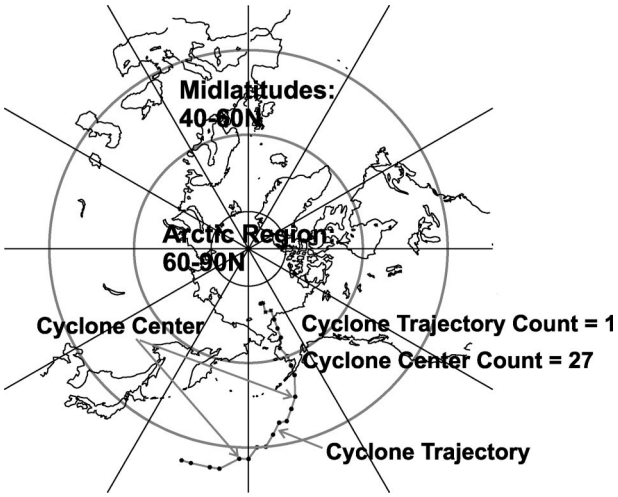

FIG. 1. A cyclone process from 0000 UTC 16 Dec to 1200 UTC 22 Dec 1999, which moves from 35.0°N, 162.5°E to 75.0°N, 165.0°W, schematically shows the difference of definitions between the cyclone trajectory count and the cyclone center count.

The homogeneity of the reanalysis fields over the central Arctic is an issue of potential concern when the study period extends back to 1948. The Russian North Pole (NP) drifting stations provided the only nearly continuous stream of SLP measurements over the central Arctic Ocean from 1950 to 1979, when the Arctic Ocean Buoy Program was initiated. Since an enhanced surface-observing network should capture pressure extrema with greater fidelity than a data-sparse network, we evaluated the temporal distribution of the most intense cyclones and anticyclones over the Arctic Ocean. The latter showed a decrease in recent decades of the reanalysis, while the former showed an increase (consistent with the overall cyclone statistics documented in the following sections). The total number of extreme synoptic systems (cyclones and anticyclones) showed no increase during the 55-yr period, implying that the capability for the detection of extreme events did not change systematically during the reanalysis period. Although this finding does not prove that the overall cyclone detection capability remained unchanged, it does give some cred-

ibility to the homogeneity of the temporal record used here.

In the Northern Hemisphere midlatitudes, rawinsonde observations had already been started by 1948, although the early upper-air observations were fewer and mainly over land. The upper-air observations for the early years actually had some advantages compared with the present day in that a number of permanent ships started observations in the late 1940s. Data at these locations continued in the northern oceans until about 1973–74 (Kistler et al. 2001). The land surface reports of surface pressure originated even earlier, for example, in the late nineteenth century in the former U.S.S.R. The total number of observations used in the reanalysis does not show a dramatic change before and after the International Geophysical Year [IGY, July 1957–June 1958; Fig. 3.1a in Kistler et al. (2001)]. The apparent change before and after the IGY is the observation time, which has been taken into account by the NCEP–NCAR reanalysis system (Kistler et al. 2001). This is in significant contrast to the Southern Hemisphere.

b. Identification and tracking of cyclones

Following Serreze (1995) and Serreze et al. (1997), we examined 6-hourly snapshots of SLP in the reanalysis data and developed the following modified empirical criteria for the identification and tracking of cyclones:

1) If the SLP at one grid point is lower than its eight surrounding grid points, a cyclone candidate is identified with its center at this grid point.
2) The minimum SLP gradient between the center of the cyclone candidate and its eight surrounding grid points is required to be at least 0.15 hPa $(100\ \text{km})^{-1}$, where the SLP values at the eight surrounding grid points are representative of spatially smoothed values of their nine surrounding grid points, respectively.
3) The minimum SLP gradient between the four surrounding points of the cyclone candidate and their outside adjacent grid points must be negative inward.
4) If cyclone candidates appear within a radius of 1200 km at the same time, they are considered to be one cyclone.
5) The cyclone track is defined as the trajectory of cyclone centers. If a cyclone's location is within a radius of 600 km of a cyclone's location at the previous 6-h time, this location is considered to be a new location of the existing cyclone. Otherwise, a new cyclone is generated. If a candidate's lifetime is shorter than 12 h, it is removed from the cyclone candidates.

The thresholds described above were found empirically. The radius used in criterion 4 is the same as in Serreze et al. (1997), which was reduced from the value in Serreze (1995). A latitudinal adjustment (sine function) was used in the SLP gradient calculation. The aim of using the minimum SLP gradient and the spatially smoothed SLP at the surrounding grid points in criterion 2 is to remove troughs extended from cyclones and to minimize the effects of irregular troughs or departures along the SLP contours in the cyclone identification. Criterion 3 serves to remove open low pressure or trough systems.

c. Parameters and an integrative index

We use cyclone center SLP and cyclone center count (number), which are defined as the SLP at the cyclone center and the number of cyclone centers over a time period (e.g., month or season), to evaluate cyclone activity on a two-dimensional grid. In addition, we define three parameters and develop an integrative index to describe *regional* characteristics of *monthly* cyclone activity.

1) Cyclone intensity is defined by the following two steps: first, the mean absolute values of the difference between the central SLP of cyclones and the climatological monthly mean SLP at corresponding grid points over the cyclone duration are calculated for each individual cyclone; second, the mean absolute values are averaged over all cyclones (trajectory count defined below) in a particular region during the month.
2) Cyclone trajectory count is the number of cyclones over the entire duration occurring in a particular region during the month.
3) Cyclone duration is defined by the following two steps: first, the mean time periods between appearance and disappearance of cyclones in a particular region are calculated for individual cyclones; second, the mean periods are averaged by the region's cyclone trajectory count.
4) Cyclone activity index (CAI) is the sum over all cyclone centers at a 6-hourly resolution of the differences between the cyclone central SLP and the climatological monthly mean SLP at corresponding grid points in a particular region during the month.

Parameters 1–3 describe a particular aspect of cyclone activity, while the integrative index represents a combination of information about cyclone intensity, trajectory count, and duration.

Climate variability is usually represented by the variance of parameters, reflecting their departures from the long-term climate mean. The departure of cyclone center SLP from the climate monthly mean SLP represents a contribution to such variance. Hence, this departure is used to represent cyclone intensity in the context of climate variability. A noteworthy distinction is the difference between the cyclone trajectory count and the cyclone center count. The former denotes the number of distinct cyclones that appeared and disappeared in the study region in each month, while the latter is a sum

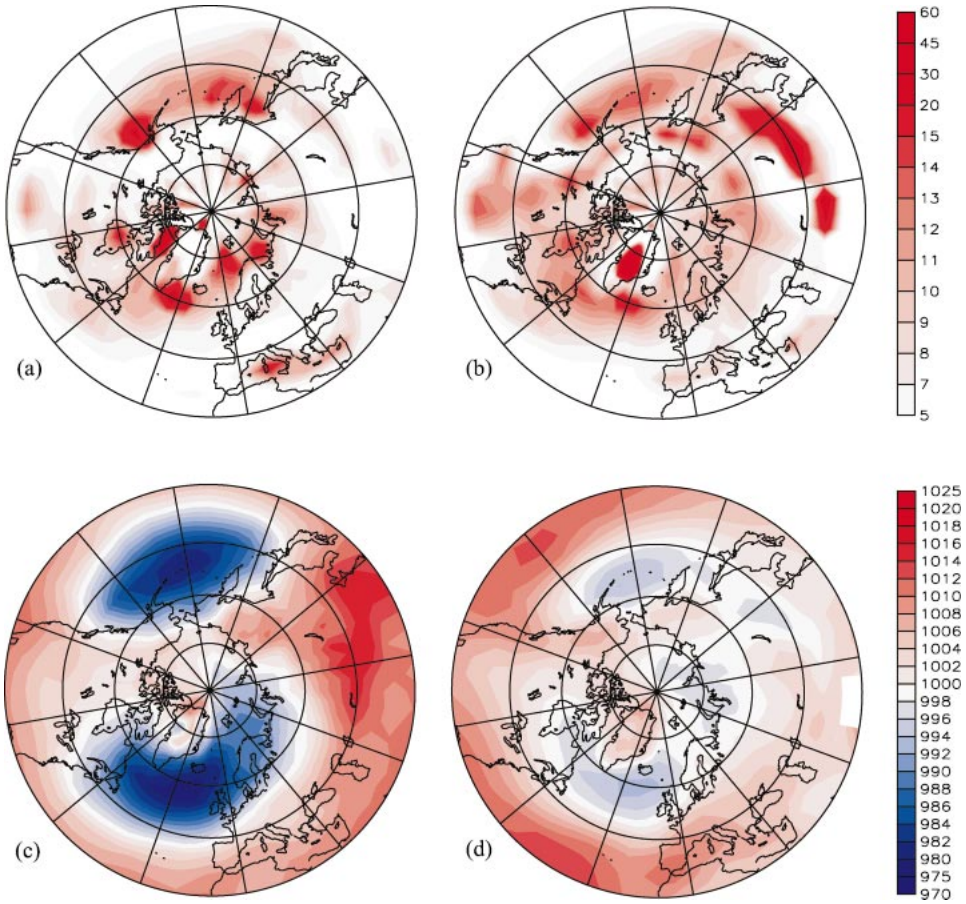

FIG. 2. The long-term mean cyclone center count in (a) winter and (b) summer; and the long-term mean SLP of cyclone centers in (c) winter and (d) summer. Panels (a) and (b) have units of counts per 10^5 km^2, and (c) and (d) have units of hPa.

of cyclone centers in the study region in all time steps of each month. The distinction is schematically explained in Fig. 1. This is a key feature of our study, distinguishing the present work from previous studies (e.g., Serreze et al. 1993, 1997; McCabe et al. 2001) in that *each cyclone is counted only once regardless of its lifetime.* Since cyclone duration is also recorded as a separate statistic, we are able to replicate the statistics of the referenced studies by combining the cyclone trajectory count and cyclone duration. We use only the CAI for interannual variability in this paper.

3. Cyclone activity climatology

a. Overall spatial characteristics

Cyclone center count and cyclone center SLP were composited into 5.0° × 5.0° grid cells to form a climatological depiction of cyclone activity in winter (October–March) and summer (April–September; Fig. 2). In order to allow for the convergence of meridians, each grid cell cyclone count was divided by the area of the grid cell to remove the influence of the varying grid cell areas.

The cyclone center count clearly shows a regional and seasonal dependence (Figs. 2a,b). The high values occur predominantly over the North Pacific and North Atlantic sectors in winter, while they are more spatially variable around the subpolar regions in summer. The areas with the maximum cyclone center count in winter range from the Sea of Okhotsk, the western Bering Sea to the Gulf of Alaska in the North Pacific and from the Greenland Sea/Iceland Sea to the Barents Sea in the North Atlantic. Baffin Bay and the Mediterranean Sea also display high cyclone center counts in winter. During summer, the high cyclone center count remains in the same region as observed in winter. It should be noted that several regions of high topography (e.g., Greenland) have artificially high cyclone frequencies because of negative biases introduced by the extrapolation of pressure to sea level.

The cyclone center SLP reflects the intensity or strength of cyclones. The geographic distribution of cyclone center SLP shows a spatial pattern very similar

TABLE 1. The total numbers of cyclones over the Arctic Ocean (north of 70°N), which are generated locally and originated south of 70°N for the winters (Oct–Mar) from 1948/49 to 2001/02 and summers (Apr–Sep) from 1949 to 2002.

			Originated south of 70°N									
	Generated locally		North Atlantic		North Pacific		Eurasia		North America			
	Winter	Summer	Winter	Summer	Winter	Summer	Winter	Summer	Winter	Summer		
Count in seasons	6860	6026	1306	1128	677	683	895	1332	364	378		
Total	12 886		2434		1360		2227		742			
						6763						

to the climatological SLP distribution, with low values occurring in the North Pacific and the North Atlantic during both winter and summer (Figs. 2c,d). This highlights the role of cyclone activity in the formation of the long-term mean of SLP. The low center SLP extends into the Arctic Ocean from the Bering Strait and the Greenland–Iceland–Norwegian (GIN) Seas.

The cyclone center SLP shows a noticeable seasonality, with lower (higher) values in winter (summer), implying deeper (shallower) cyclones. The SLP is remarkably high over Eurasia in winter and the midlatitude oceans in summer, reflecting the dominance of the continental high during winter and subtropical highs during summer. Not surprisingly, the areas of high SLP collocate with low cyclone center counts. The seasonal variation of the SLP over the continents is stronger than over the oceans. The SLP over Eurasia dramatically decreases from winter to summer as the cyclone center count increases.

Although the cyclone center count over the Arctic Ocean is generally lower than that over the subpolar regions, lower center SLP values exist in the Arctic Ocean year-round, and there is still a considerable number of cyclones generated locally over the Arctic Ocean or migrating from lower latitudes to the Arctic Ocean during the study period. The breakdown of cyclone center counts based on origins and seasons is shown in Table 1. The midlatitudes are divided into four sectors: the North Atlantic (70°W–20°E), the North Pacific (140°E–120°W), Eurasia (20°–140°E), and North America (120°–70°W).

We assembled all tracks of cyclones that reached the Arctic Ocean during the last 54 winters and summers and found that seasonal differences are evident (not shown). There are more cyclones originating in the midlatitudes propagating into the Arctic Ocean in winter than in summer. In particular, the northward-propagating cyclones during winter are concentrated in three pathways: from the northwestern Pacific Ocean to the Bering Strait/Chukchi Sea, from the North Atlantic Ocean to the GIN Sea/Barents Sea, and from northern Europe to the Eurasian shelf seas. This is consistent with Whittaker and Horn (1982). However, the cyclone tracks are diverse around the subpolar regions in summer and no dominant pathway is evident. The cyclone tracks are in good agreement with the spatial distribution of cyclone center count in Figs. 2a,b.

b. Arctic regional analysis

1) CYCLONE INTENSITY, COUNT, AND DURATION

The cyclone intensity is greater during the cold season (October–April) than the warm season (March–September) throughout the Arctic region, with a maximum (minimum) in February (July; Fig. 3a). Recall that the intensity is defined as the magnitude of the departure from the climatological monthly mean SLP at a grid point. Regional differences are evident, particularly in winter when cyclones in the Arctic marginal zone are up to 3.0 hPa deeper than those over the Arctic Ocean. During summer, cyclones are about 1.5 hPa deeper over the Arctic Ocean than the Arctic marginal zone. The seasonal amplitude is larger in the Arctic marginal zone.

Cyclone trajectory count displays only a modest seasonal cycle (Fig. 3b) characterized by slightly more cyclones in summer than winter in the Arctic marginal zone. Serreze et al. (1997) observed higher cyclone center counts in the Icelandic low region in winter. This apparent inconsistency evidently results from a combination of 1) the different definitions of cyclone trajectory count and cyclone center count, and 2) domain area, as our Arctic marginal zone encompasses all longitudes, not merely the Icelandic sector. The cyclone trajectory count in the Arctic Ocean shows little seasonal variability.

The duration of cyclones in both the Arctic marginal zone and the Arctic Ocean is longer during summer than winter, with maximum values occurring in July and June (Fig. 3c). In particular, the cyclones in the Arctic Ocean show a noticeably longer duration during summers. However, comparison of the duration between the Arctic Ocean and the Arctic marginal zone is difficult to interpret. The longer duration in the Arctic Ocean than the Arctic marginal zone could reflect the different proportions of lifetime in the two areas, or the different migration speed of cyclones in respective regions, that is, it could indicate that slow-moving occluding systems tend to be found in the Arctic Ocean.

2) INTENSITIES OF CYCLONES WITH DIFFERENT ORIGINS

As indicated in section 3a, cyclones occurring in the Arctic region can be generated locally or can originate in lower latitudes. In the climatic mean, there are about

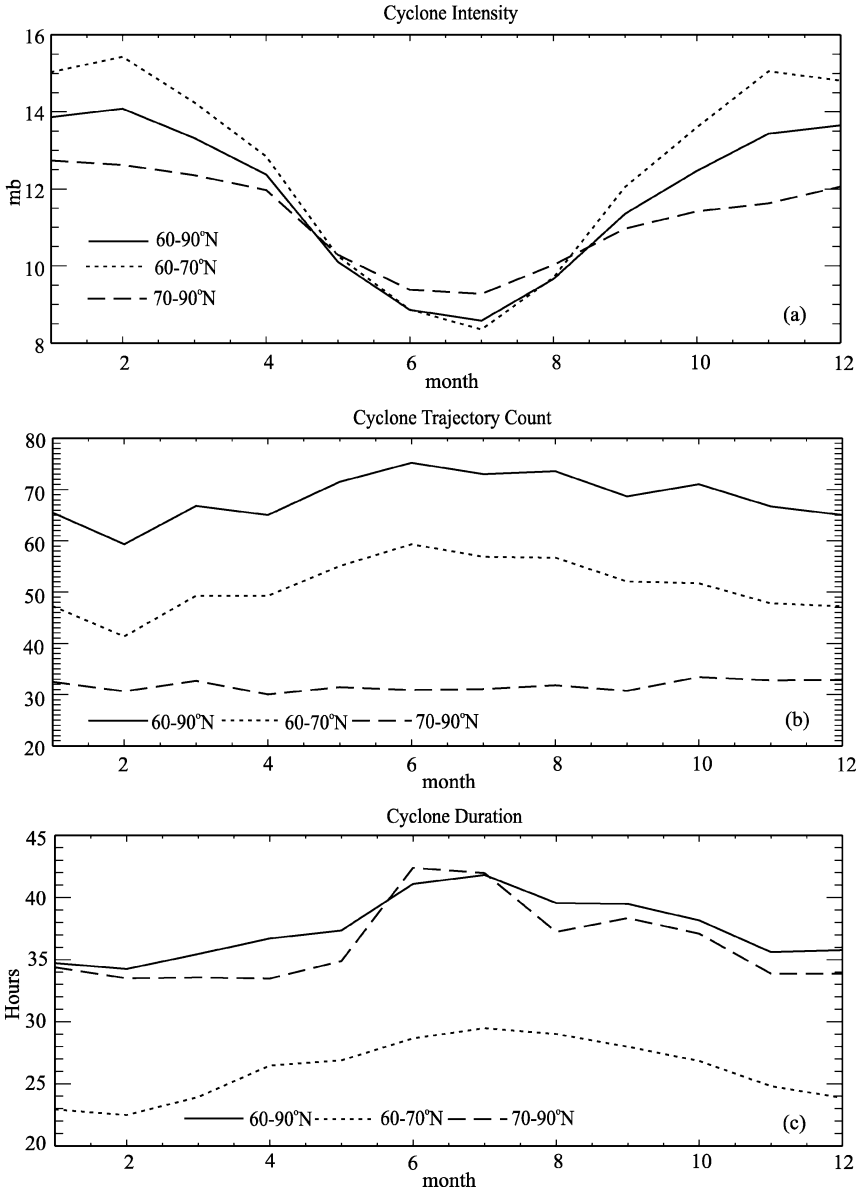

FIG. 3. The long-term mean seasonal cycle of cyclone (a) intensity, (b) trajectory count, and (c) duration in the Arctic region (60°–90°N) and its two subregions, the Arctic Ocean (70°–90°N) and the Arctic marginal zone (60°–70°N). The units of intensity and duration are in hPa and h, respectively.

50 cyclones born annually in the Arctic region (60°–90°N) and about 17 cyclones coming from subpolar areas or midlatitudes in each month. Serreze et al. (2001) depicted the distribution of counts of cyclogenesis over the Arctic region and showed a sharp seasonal contrast between summer and winter. During winter, the most cyclogenesis occurs east of Greenland, over the Barents Sea and in the Baffin Bay and western Canada while, during summer, the most cyclogenesis appears over east-central Eurasia and Alaska. Cyclones generated over the Eurasian Arctic tend to track eastward with most of them entering the Arctic Ocean. However, cyclones generated over Alaska primarily track southeastward into the Canadian Arctic Archipelago.

Considering the large difference between the cyclone counts generated locally over the Arctic region and remotely in the midlatitudes, we only plot the cyclone intensities to examine the dependence of intensity on region or origin (Fig. 4). The cyclones are generally more intense in winter and weaker in summer. Cyclones generated in the Arctic region are less intense than those from lower latitudes. Cyclones from the North Atlantic have the greatest intensity over the entire year, while those from the North Pacific exhibit the least strength

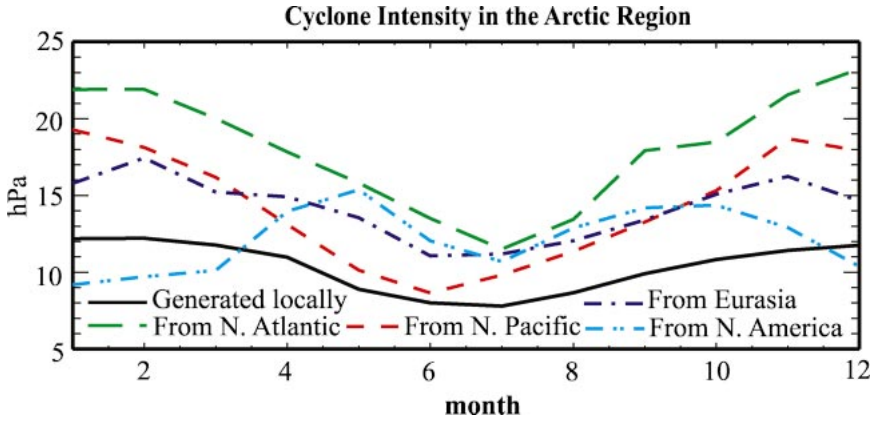

FIG. 4. The seasonal cycle of the intensity (number of hPa below climatological mean) of cyclones that are generated locally in the Arctic region (60°–90°N) and those that propagate into the Arctic region through the North Atlantic, the North Pacific, Eurasia, and North America.

in summer. Cyclones originating over North America tend to have two peaks and are more intense during the warm months, with maximum intensity values in May and September. Cyclones from Eurasia display a maximum intensity in February and November. Additionally, the cyclones originating over the oceans have a larger seasonal amplitude than those from the continental area.

The results above indicate that cyclones in the Arctic region tend to be more intense, shorter lived, and fewer in number in winter, while they are less intense, longer lived, and more numerous in summer. The cyclone intensity differs based on the region of origin. Generally, cyclones originating in lower latitudes are stronger than those generated locally. The cyclones coming from the North Atlantic are stronger than those from the other low-latitude sectors.

4. Interannual variability of cyclone activity in the Arctic region

a. Integrated cyclone activity—CAI anomalies

Trends and interannual variability of the CAI anomaly are visually apparent in the Arctic region (Fig. 5), in which all calendar months are included and a 13-point smoother is applied to highlight the interannual variability. The CAI anomaly appears to increase with time, showing a dominance of negative anomalies in the 1950s–60s and positive anomalies in the 1990s, respectively. Superimposed on the trends, the CAI anomaly shows notable fluctuations interannually, with relatively small amplitudes in the 1950s and 1980s and relatively large amplitudes in the 1960s–70s and the 1990s. In particular, the fluctuation of the CAI anomaly for the Arctic region was dramatically amplified during the period 1988–90, indicating strengthened cyclone activity during this period, which is consistent with the behavior of the AO index.

The variations of CAI anomaly in the Arctic Ocean and the Arctic marginal zone show in-phase and out-of-phase relations in different periods. Consistent variations of the CAI anomaly in both subregions occurred during the periods from the 1960s to the mid-1970s and from the mid-1980s to the early 1990s, when the CAI anomalies in the Arctic region and in the two subregions were amplified. In particular, during the latter period, the variations of the CAI anomaly in both the subregions were well synchronized and intensified, suggesting a resonance-like interaction of the CAI anomalies in these two subregions. On the other hand, opposite changes of CAI anomalies in these two subregions occurred in the 1950s, from the late 1970s to the mid-1980s, and in the mid-1990s, during which the amplitude of the CAI anomalies in the entire Arctic region was suppressed. A running correlation analysis with a moving 72-month window of the CAI anomalies between the Arctic Ocean and the Arctic marginal zone shows a significant correlation coefficient of 0.95 from 1987 to 1988, indicating a reinforcing interaction of the CAI anomalies between these two subregions. Rogers (1990) and Clark et al. (1999) reported that cyclones in the North Atlantic migrate toward the interior of the Arctic Ocean in the positive North Atlantic Oscillation (NAO), while cyclone tracks orient zonally along 40°–45°N over Europe and southwestern Asia in the negative NAO, which could be a synoptic manifestation of these interactions.

b. Spectral features of the integrated cyclone activity

Spectral analysis can help us better understand the dominant temporal components of the variability and may provide predictive skill for cyclone activity. The multitaper method (MTM) of spectral analysis provides an optimally low-variance, high-resolution spectral estimate (Mann and Lees 1996; Ghil et al. 2002). The assumptions of this method regarding signal (narrowband, but not strictly periodic) and noise (''red'') are appropriate for climate applications, and the method is

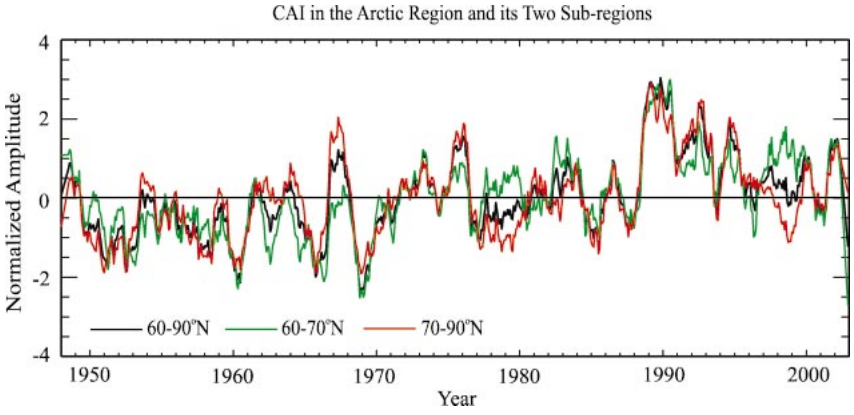

FIG. 5. The CAI anomalies for the Arctic region (60°–90°N) and its two subregions, the Arctic Ocean (70°–90°N) and the Arctic marginal zone (60°–70°N), to which the 13-point smoother has been applied.

''robust'' for accurately determining the noise component of the spectrum. We made spectral estimates of the CAI in the Arctic region by the MTM and reconstructed dominant low-frequency components of the CAI variability.

The CAI anomalies exhibit significant low-frequency variation (called ''secular trend'' by Ghil et al. 2002) and periodical signals on interannual time scales in the Arctic region (Fig. 6a) corresponding to the three-peak spectra in Table 2. The reconstructed low-frequency variation shows a slow evolution of the CAI from a negative phase to a positive phase from 1948 to 2002, with extreme low and high values in the early 1960s and early 1990s, respectively (Fig. 6b). The point of inflection occurs around 1976. The contribution of the low-frequency variation to the cyclone variability is considerable. Its maximum normalized amplitude is 0.8σ. This mode is consistent with the low-frequency changes in NAO activity (Dickson et al. 2000) and Arctic air temperatures (Polyakov et al. 2002). Moreover, the point of inflection in 1976 also coincides with the phase transition time of the Pacific decadal oscillation (PDO) from a cold to warm episode, and the low-frequency variation of the CAI anomaly corresponds well to the low-frequency change of the PDO index (Trenberth and Hurrell 1994). It is possible, although by no means proven, that increasing greenhouse gas concentrations have been a contributing factor to the 1976 phase transition and subsequent changes (Houghton et al. 2001).

The other two dominant low-frequency signals are the oscillations with periods of 7.8 and 4.1 yr, which are significant at the 99% levels. The 7.8-yr oscillation is amplified during the periods from the late 1940s to the early 1960s and from the early 1970s to the early 1990s, while it is suppressed in the 1960s and trends to be weakening in the 1990s (Fig. 6c). The 4.1-yr fluctuation is more energetic from the 1960s up to 1980 and in the 1990s, while it is relatively weak in the 1960s and 1980s (Fig. 6d).

Comparisons of Figs. 6b–d indicate that interactions of these three dominant spectral components can explain much of the CAI variation. The three representative periods (1: 1988–91), (2: 1976–81), and (3: 1968–71) can illustrate such interactions, which together contribute to an amplified positive anomaly, a weak/flat anomaly, and a maximum negative anomaly of CAI, respectively. For example, in period 1 the low-frequency variation and the 7.8- and 4.1-yr oscillations are all in their positive phase with the latter two oscillations reaching maximum values. A composite of these three signals is consistent with the pronounced amplification of the CAI anomaly around 1990. Similarly, the CAI anomalies are a consequence of canceling and reinforcing negative values of these three signals in periods 2 and 3.

The 7.8-yr oscillation seems to dictate the regime alternation of the Arctic sea ice and ocean motion, particularly when it is robust. As a consequence of atmospheric forcing, two regimes of Arctic sea ice and ocean motion were proposed by Proshutinsky and Johnson (1997). Anticyclonic wind-driven ice and ocean motion in the central Arctic were assigned by Proshutinsky and Johnson to the years 1946–52, 1958–62, 1972–79, and 1984–88, and cyclonic motion to the years 1953–57, 1963–71, 1980–83, and 1989–93. When comparing these time periods with our spectral analysis, the anticyclonic and cyclonic regimes are in general agreement with the 7.8-yr oscillation, although the correlative relationship is lost in the 1970s when the 7.8-yr oscillation is weak. The relationship between the 7.8-yr oscillation and Arctic sea ice and ocean motion may also provide an interpretation of large-scale atmosphere–sea ice–ocean interaction and a very general predictive skill for sea ice and ocean changes. It is perhaps noteworthy that Proshutinsky and Johnson's estimate of time scale is slightly different from the 7.8-yr estimation. This could be caused by the mix of other significant signals in the real climate system. The different methodologies in Proshutinsky and Johnson's (1997) and our studies make

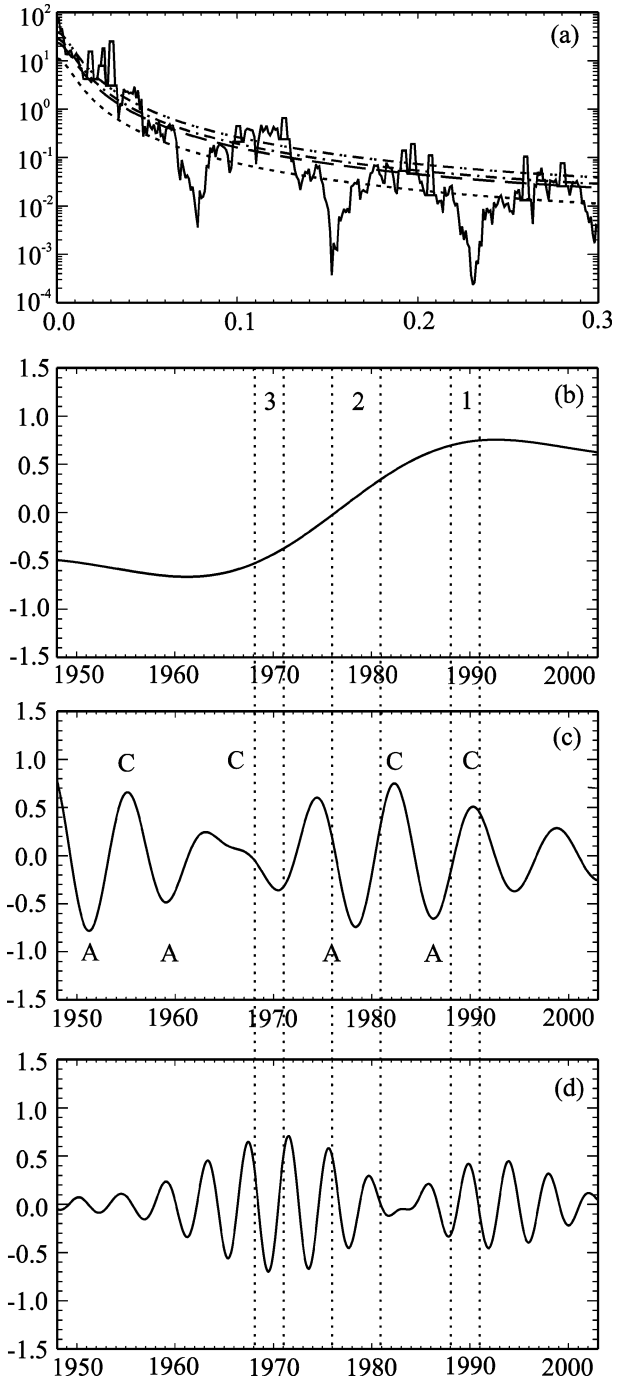

FIG. 6. (a) The MTM spectrum of the CAI anomaly time series for the entire Arctic region. The estimated red noise background and associated 90%, 95%, and 99% significant levels are shown by the short-dashed, the long-dashed, the dot–dashed and the double dot–dashed curves, respectively. The *x* coordinate is the frequency in cycles per month and the *y* coordinate is the spectrum. The bandwidth parameter $p = 2$, and three tapers were used. (b)–(d) Reconstructed signals of the low-frequency variation and 7.8- and 4.1-yr oscillations. The numbers 1–3 in (b) represents three selected representative periods, which are bounded by the dashed lines from (b) to (d). The letters ''C'' and ''A'' represent the cyclonic and anticyclonic regimes of sea ice and ocean motion defined by Proshutinsky and Johnson (1997).

TABLE 2. Significant low-frequency signals in the CAI variability for the Arctic region, estimated by MTM.

Spectrum	Significant level	Period
0.0010	99%	Low-frequency
0.0107	99%	7.8 yr
0.0205	99%	4.1 yr

it impossible to do quantitative correlation analysis of two time series.

5. Contributions by cyclones with midlatitude origins

a. Relationship of cyclone activity between the Arctic region and the midlatitudes

1) CAI ANOMALIES

The CAI anomalies were calculated in the entire midlatitude area and its four longitudinal sectors. They show three distinct periods of alternating upward and downward tendencies of the index (Fig. 7a). From 1948 to

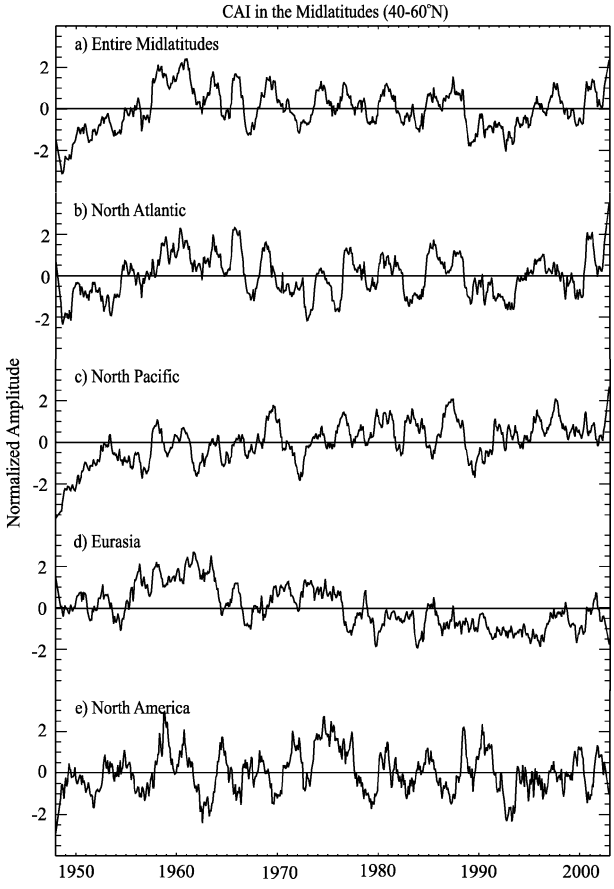

FIG. 7. The CAI anomalies in (a) the entire midlatitudes and its four sectors, (b) the North Atlantic, (c) the North Pacific, (d) Eurasia, and (e) North America.

TABLE 3. Correlation coefficients of the CAIs between the Arctic region and the midlatitudes. Correlation significant at the 99% confidence level is in bold.

	Midlatitudes				
CAI	Entire band	North America	North Atlantic	Eurasia	North Pacific
Arctic	**−0.452**	**0.104**	**−0.461**	**−0.421**	−0.036

1960, the CAI anomaly increases, implying intensified cyclone activity. Subsequently, from 1960 to 1992, the CAI anomaly decreases gradually and the cyclone activity weakens. The minimum midlatitude CAI anomaly occurs between 1989 and 1993. Since 1993, the CAI has increased to a positive phase. The CAI anomalies in the midlatitudes and the Arctic region show generally opposite variations, with a remarkable contrast occurring from 1988 to 1991, as shown by the significant negative correlation in the first column in Table 3.

The CAI anomalies in the four midlatitude sectors show significant differences in interannual variations (Figs. 7b–e) despite their positive trends from 1948 to 1960. After 1960, the CAI anomalies in Eurasia show a linear decreasing variation, while the CAI anomalies in the other three sectors exhibit interannual and decadal fluctuations. In particular, the CAI anomalies in Eurasia, the North Atlantic, and the North Pacific are in their maximum negative phases around 1990, as opposed to that in the Arctic region. The CAI anomaly in the North American sector is in its positive phase. Cross correlation coefficients reveal that the negative correlation between the Arctic region and the midlatitudes is strongest in the North Atlantic and Eurasian sectors (Table 3).

The increases of CAI anomalies in the early decade may cause concern due to the data availability prior to IGY. In section 2a we discussed that there is no apparent dramatic increase of observations from 1948 to 1960, in significant contrast to the Southern Hemisphere. Thereafter, we believe that the increase of cyclone activity in the midlatitudes could be caused by physics rather than by changes in the observation network. Particularly, there are large numbers of surface reports over Eurasia dating back to the late nineteenth century. The CAI anomalies over Eurasia exhibit a clear increase from 1948 to the early 1960s, long after surface reports became numerous.

2) VIEWS FROM THE MOST SIGNIFICANT LOW-FREQUENCY SIGNALS OF THE CAI ANOMALIES

Figure 8 shows the most significant low-frequency signals in the midlatitude sectors. The signal in the North Atlantic leads that in North America. The former has its extreme positive phase around 1962 and a negative phase around 1985, while the latter has a maximum value in 1975. Lin and Derome (1998) also found a significant lagged correlation of winter mean atmospheric anomalies between the North Atlantic Ocean (leading) and North America (lagging). Their results show a 3-yr phase difference. Nevertheless, the cyclone activity exhibits a phase difference of about 13 yr in our results. The mechanism for this lagged correlation remains an open question. The most significant low-

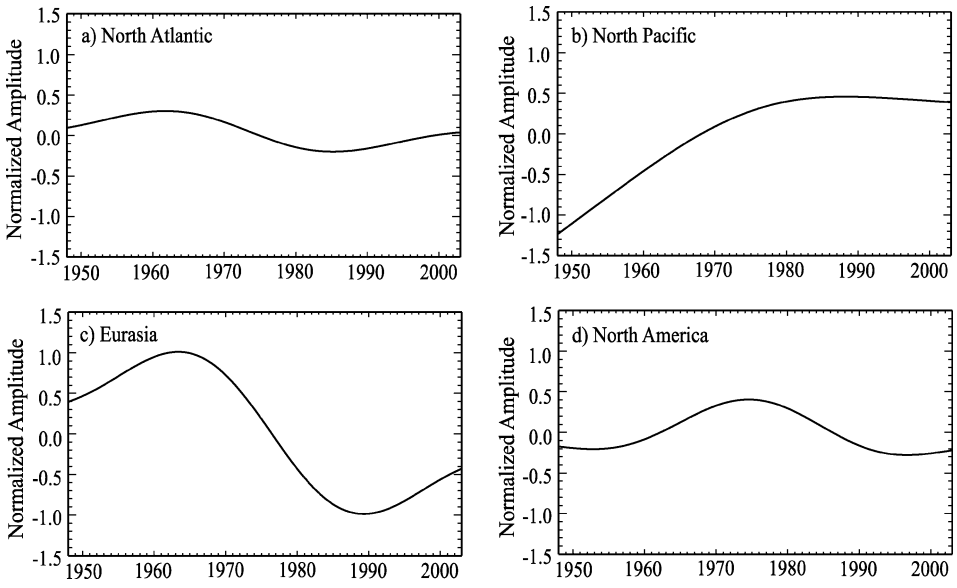

FIG. 8. The most significant low-frequency variation signals of CAI anomalies as determined by the MTM spectral analysis in the four midlatitude sectors: (a) the North Atlantic, (b) the North Pacific, (c) Eurasia, and (d) North America. The signals in (a)–(c) are significant at the 99% level and the signal in (d) is significant at the 95% level.

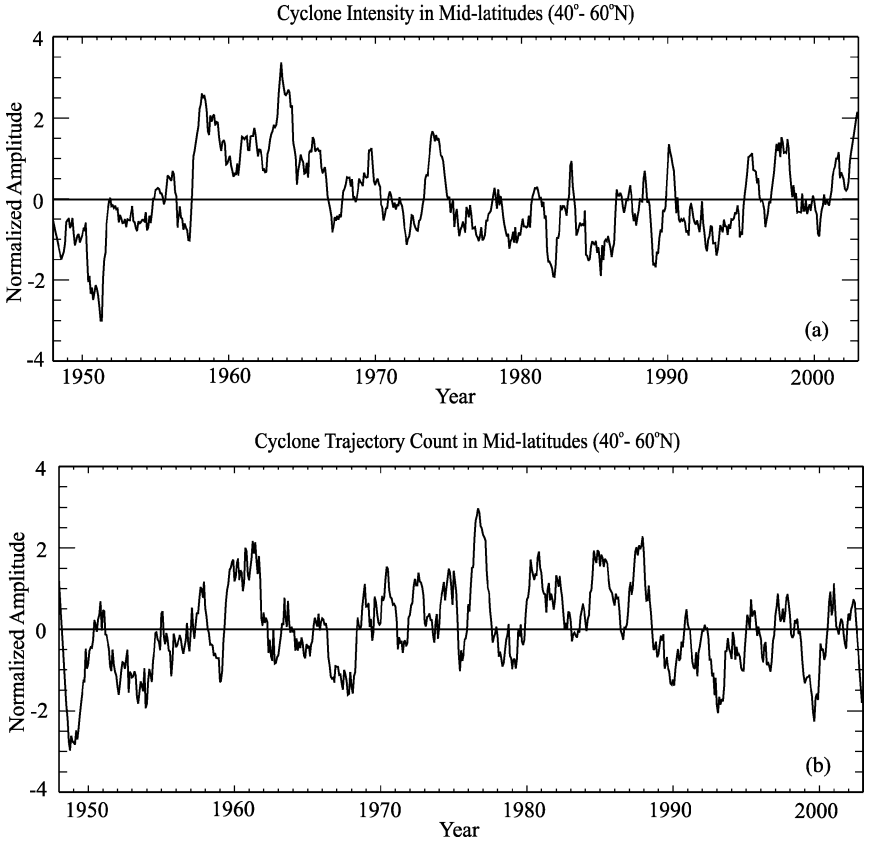

FIG. 9. The anomalies of (a) cyclone intensity and (b) cyclone trajectory count in the entire midlatitude area.

frequency signals in Eurasia and the North Atlantic are similar, with positive values in the 1960s and negative values in the 1980s. The signal in Eurasia has the largest amplitude variation among the four sectors relative to climatology (CAI anomalies in Eurasia, the North Atlantic, and the North Pacific have comparable standard deviations). The signal in the North Pacific shows an almost linear increasing tendency from 1950 to 1980 and then remains relatively steady. Graham and Diaz (2001) found that the frequency and intensity of extreme cyclones have increased markedly in the North Pacific Ocean in winter (December–March), which is consistent with our results described here by the CAI and represented by the lowest-frequency signal in Fig. 8b.

The negative correlation of CAI anomalies between the Arctic region and the midlatitude North Atlantic and Eurasia shown in Table 3 can be deduced from a comparison of the most significant low-frequency signals between Fig. 6b and Figs. 8a and 8c. In particular, the signal in Eurasia is nearly the opposite of that in the Arctic region. This accordingly suggests that the poleward shift of cyclone activity proposed by Serreze et al. (1997) and McCabe et al. (2001) may have resulted primarily from changes in the Eurasian and North Atlantic sectors.

3) CAI COMPONENT INFORMATION: CYCLONE INTENSITY AND TRAJECTORY COUNT

We examined the cyclone intensity, trajectory count, and duration, thereby decomposing the integrated information in the CAI. The duration shows minor correlations with the CAI anomalies, so we focus here on intensity and trajectory count. The cyclone intensity in the entire midlatitude area generally increased before the mid-1960s, then decreased until the late 1980s (Fig. 9a). A gradual recovery occurred in the 1990s. The cyclone trajectory count shows two periods with noticeable increasing tendencies: before the early 1960s and from the late 1960s to the late 1980s. A sharp drop occurs around 1988–90 (Fig. 9b), a period corresponding to the intensification of the Arctic cyclones (Fig. 5) and the amplification of the AO mode. The variation of cyclone center count is very similar to that of the cyclone trajectory count rather than cyclone duration, suggesting that the cyclone trajectory count plays an important role in the midlatitudes. Comparisons of Figs. 9 and 10 indicate that the long-term variations of the cyclone intensity and trajectory count in the midlatitudes are dominated by those in Eurasia, while the drop of cyclone trajectory count in the North Atlantic also makes some contributions.

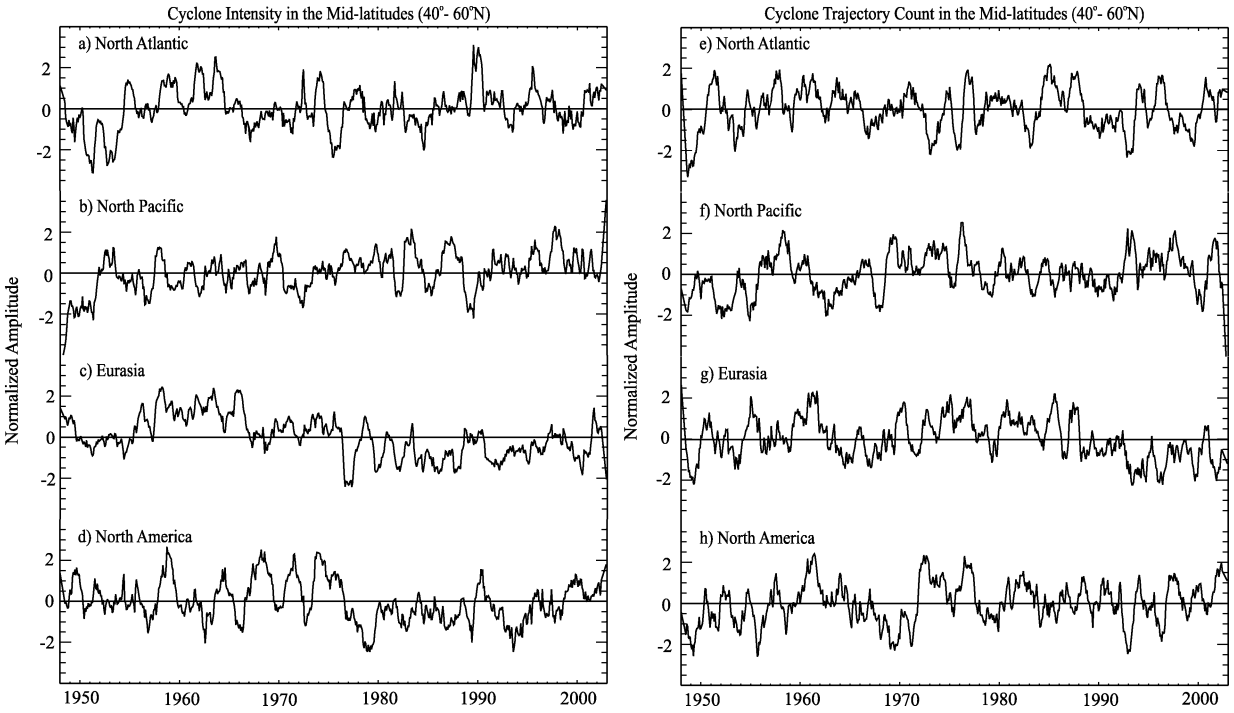

FIG. 10. The anomalies of cyclone intensity in (a) the North Atlantic, (b) the North Pacific, (c) Eurasia, and (d) North America. The anomalies of cyclone trajectory count in (e) the North Atlantic, (f) the North Pacific, (g) Eurasia, and (h) North America.

The contribution to the CAI anomalies by the cyclone intensity and trajectory count interaction can be seen clearly by comparing Figs. 7a and 9. In particular, the cyclone trajectory count played a dominant role in the maximum negative anomalies of CAI from 1988 to 1992. Such a contribution in midlatitude subregions can also be seen by comparing Figs. 7b–e and 10. For example, the cyclone intensity anomalies are stronger while the cyclone trajectory count anomalies are smaller in the North Atlantic during 1989–91. Predominance of the cyclone trajectory count's contribution to the CAI leads to a negative CAI anomaly, that is, fewer stronger cyclones can still result in negative CAI anomalies.

Correlations in Table 4 quantify the relationship of the cyclone activity between the Arctic region and different midlatitude sectors. Negative correlation coefficients occur between the CAI in the Arctic region and both the intensity and trajectory count in midlatitude Eurasia, while positive correlations are found between the CAI in the Arctic region and the intensity in the midlatitude North Atlantic. Given the close similarity between the cyclone trajectory count and the center count in the midlatitudes, the results suggest that McCabe et al.'s (2001) finding of decreased cyclone center count and increased cyclone intensity is primarily true in the North Atlantic. Our results also indicate that the fluctuations dominated trends of cyclone trajectory counts over much of the 55-yr period, with the major exceptions being the most recent 20 yr in the North Atlantic and Eurasia. There is no apparent negative trend of cyclone trajectory count in the North Pacific and North America. The cyclone intensities showed decreases from 1960 to 1990 in Eurasia and North America, while no obvious trends were evident in the North Atlantic and Pacific except a strong amplification in the North Atlantic during the late 1980s.

TABLE 4. Correlation coefficients between the CAI in the Arctic region and cyclone intensities and trajectory counts in the midlatitudes. Correlation significant at the 99% confidence level is in bold.

	Intensities (upper) and trajectory counts (lower) in midlatitudes			
	North America	North Atlantic	Eurasia	North Pacific
CAI in the Arctic	−0.008	**0.188**	**−0.205**	−0.057
	0.155	**−0.442**	**−0.302**	0.005

b. Relations between cyclone origins and the Arctic cyclone activity

The intensities of the cyclones born in the Arctic region and of those originating equatorward of 60°N display a complex relationship over the study period (Fig. 11a). An increase of intensities occurred from the late 1980s to the early 1990s, suggesting that both types of cyclones contributed to the amplification of CAI anomalies (Fig. 5). In contrast, the intensities of two types of cyclones exhibited an out-of-phase relationship in the 1970s and 1990s. In particular, the cyclones orig-

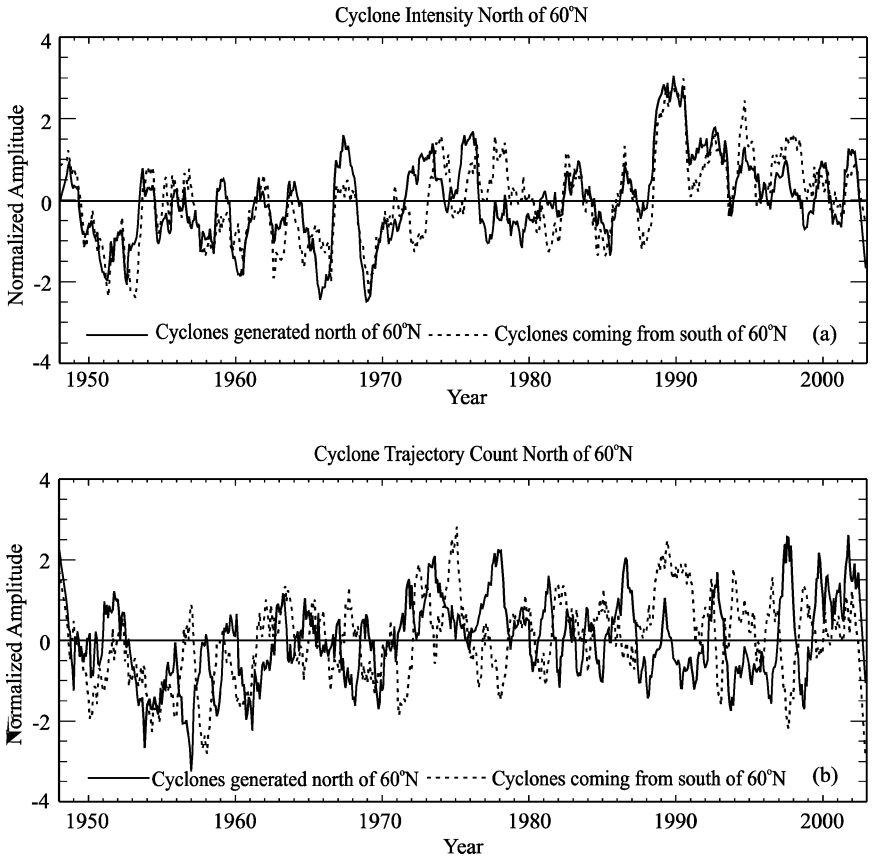

FIG. 11. The cyclone (a) intensity and (b) trajectory count anomalies in the Arctic region (60°–90°N). The cyclones are separated into two parts: those that are generated in the Arctic region (north of 60°N) and those that originate in lower latitudes (south of 60°N).

inating in lower latitudes were in their high phase during 1977–81, while at the same time the cyclones generated in the Arctic were in an anomalous lower phase. Conversely, the cyclones generated locally remained in their positive phase during 1991–93, but the cyclones coming from the south showed a rapid decrease. The cyclones from the south did not support the maintenance of the large anomaly that developed around 1990.

The trajectory counts of cyclones originating in the two regions also show signatures consistent with the CAI variability in the Arctic region (Fig. 11b). Specifically, there was a generally increasing tendency from 1955 to 1980 and a decreasing tendency after 1980 for both types of cyclones. The fluctuations were amplified in the late 1980s. However, the phasing of the increases of cyclones that originated locally and in the midlatitudes shows distinct differences. Cyclones formed within the Arctic showed several spikes, followed by rather rapid decays. Cyclones that originated south of 60°N increased sharply around 1988, and their counts remained high through 1991. Thus the trajectory count of cyclones that originated in the lower latitudes tends to support the CAI anomaly persistence in the Arctic region during 1988–91, while the cyclones generated locally favor the decay of the positive CAI anomalies.

When examining other periods in Fig. 11b, we find that the variations of trajectory counts of cyclones propagating into the Arctic region, and cyclones generated within the Arctic region were frequently out of phase. Such relationships are especially apparent in the 1970s and 1990s. For example, from 1977 to 1981, the trajectory count of cyclones generated locally was anomalously positive while the trajectory count of cyclones originating in lower latitudes was anomalously negative. Opposing variations of these two types of cyclones contributed to the weak CAI anomaly.

The features of the cyclone intensity and cyclone trajectory count shown in Fig. 11 also vary regionally. It is intriguing that cyclones from all four midlatitude sectors intensified from 1988 to 1991 (Figs. 12a–d). Specifically, the intensities of cyclones from the North Atlantic, Eurasia, and the North Pacific were substantially amplified and synchronized in 1988–89, though the North American increase occurred later, in 1990–91. The intensities of cyclones from the North Atlantic and Eurasia have the largest amplitudes and remain anom-

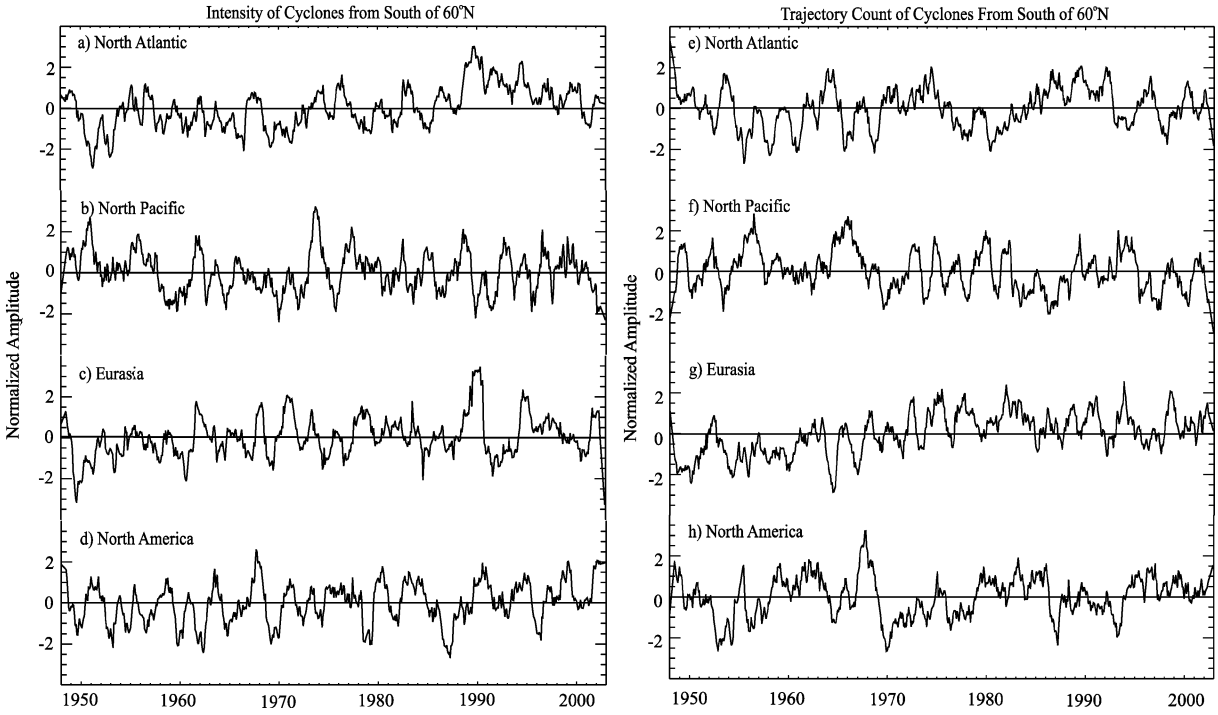

FIG. 12. The anomalies of cyclone intensity originating south of 60° and passing through 60°N in (a) the North Atlantic, (b) the North Pacific, (c) Eurasia, and (d) North America. The anomalies of cyclone trajectory count originating south of 60° and passing through 60°N in (e) the North Atlantic, (f) the North Pacific, (g) Eurasia, and (h) North America.

alously positive for a longer time. However, the decay rates differ among the various sectors. The cyclones from the North Atlantic after 1990 remained in the higher positive phase longer than others.

With respect to the trajectory counts of cyclones entering the Arctic from different regions, Figs. 12e–h show an increasing amount of cyclones from Eurasia before 1975. After that time, the cyclone trajectory count remains in the positive anomaly phase. The trajectory count of cyclones from the North Atlantic displayed decadal fluctuation with positive anomalies mainly from 1970 to 1975 and from 1987 to 1992 and negative anomalies from 1955 to 1969 and from 1976 to 1986. The trajectory counts of cyclones from Eurasia and the North Atlantic showed positive anomalies from the late 1980s to the early 1990s. This demonstrates that there were more cyclones entering the Arctic Ocean through these two sectors at that time, although Figs. 10e,g indicate that there were fewer cyclones in the corresponding regions in the midlatitudes. Consequently, cyclones from the Eurasian and North Atlantic sectors showed the closest ties to Arctic cyclone activity during the period of AO intensification around 1990.

6. Composite analysis based on CAI extremes in the Arctic

We analyzed Arctic cyclone activity and its relationship to the midlatitude cyclone activity in a regionally integrated way. In order to better understand how spatial changes of cyclone activity in the Arctic and midlatitudes are coordinated, we constructed composites of the cyclone center count (Fig. 13) and the cyclone center SLP (Fig. 14) for the winters and summers in which the magnitude of the seasonal mean CAI anomaly exceeded 1.0σ. This bridges cyclone activity statistics and large-scale climate variability. The selected winters and summers in the positive and negative phases are listed in Table 5. The selected years of the positive (negative) phase occurred mainly after (before) 1970, which suggests increasing cyclone activity in the last 30 yr.

The overall spatial patterns of the cyclone center count for the extreme phases compare favorably with the long-term climate mean (Figs. 2a,b). However, a poleward shift of storm tracks in the North Atlantic and significant enhancements of the cyclone center count are apparent, particularly in summer. During winter, positive CAI anomalies are associated with increased cyclone center counts in the Canada Basin, the Beaufort and Chukchi Seas, and the Laptev Sea. The cyclone center count also increases in the zonal band between 60° and 70°N, particularly over the Greenland Sea and the Iceland Sea. However, the cyclone center count decreased in the subpolar regions between 40° and 60°N, with maximum reductions occurring in the climatological storm track regions of the North Atlantic and North Pacific. During summer, the increase of the cyclone center count is stronger and the area of increase is more

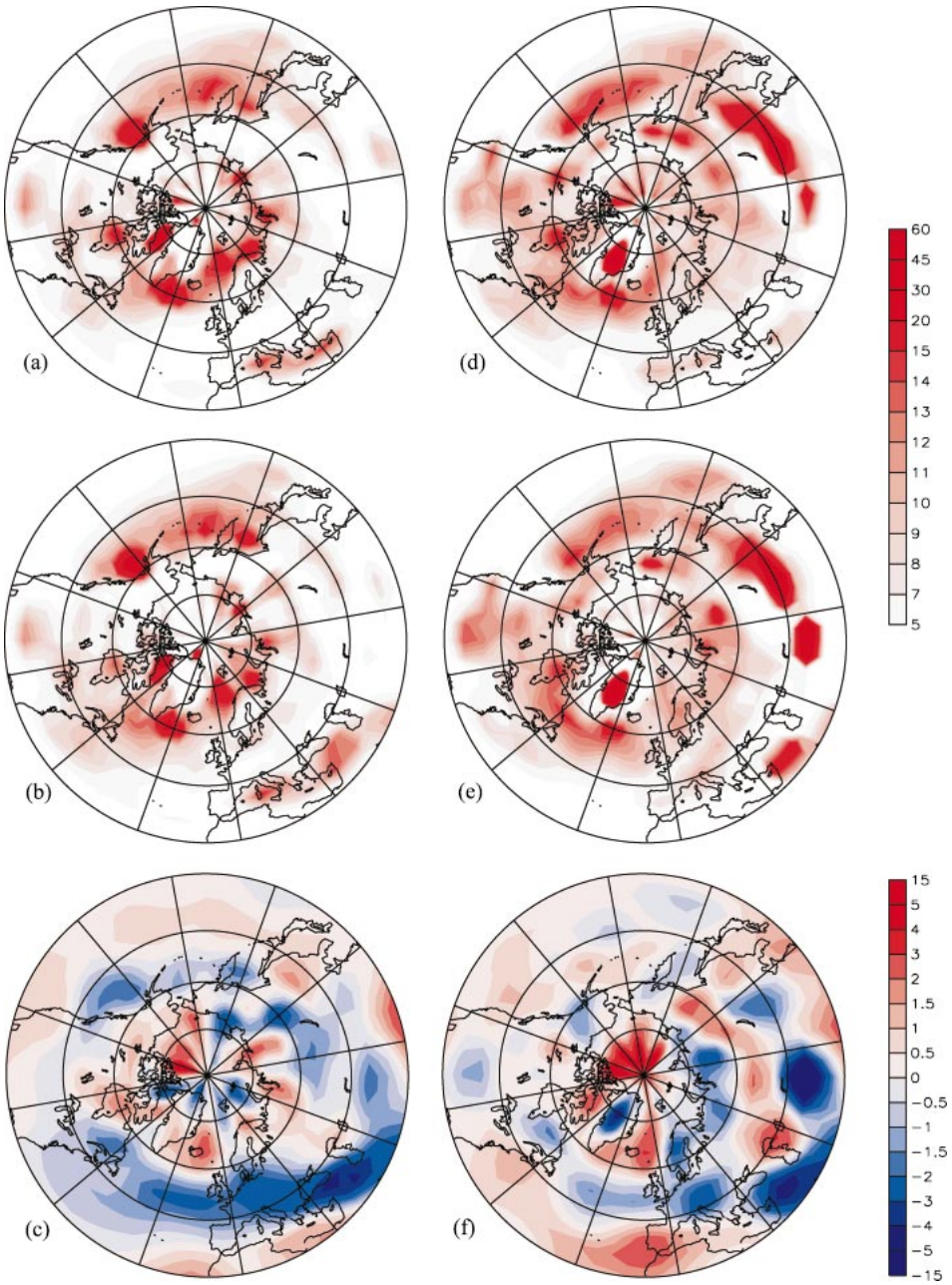

FIG. 13. The composite cyclone center count in the winters with the CAI anomalies (a) larger than 1.0 std dev, (b) less than −1.0 std dev, and (c) their difference. The composite cyclone center count in the summers with the CAI anomalies (d) larger than 1.0 std dev, (e) less than −1.0 std dev, and (f) their difference.

poleward than in winter over the Arctic Ocean. The area of reduced cyclone center count also contracts northward, with the maximum decrease occurring along the Eurasian coast of the Arctic Ocean. However, a belt of increasing cyclone count extends from the Caspian Sea to eastern Asia between 40° and 65°N in Eurasia. Serreze et al. (1997) reported increased cyclone frequency north of the Canadian Archipelago in winter when the NAO phase was positive (their Fig. 8), which is consistent with our Fig. 13c.

Correspondingly, the cyclone center SLP drops markedly in the Arctic region but rises in the midlatitudes when the CAI anomaly changes from negative to positive. This implies deeper cyclones in the Arctic region and shallower cyclones in the midlatitudes when the CAI anomalies are positive. The SLP decrease occupies

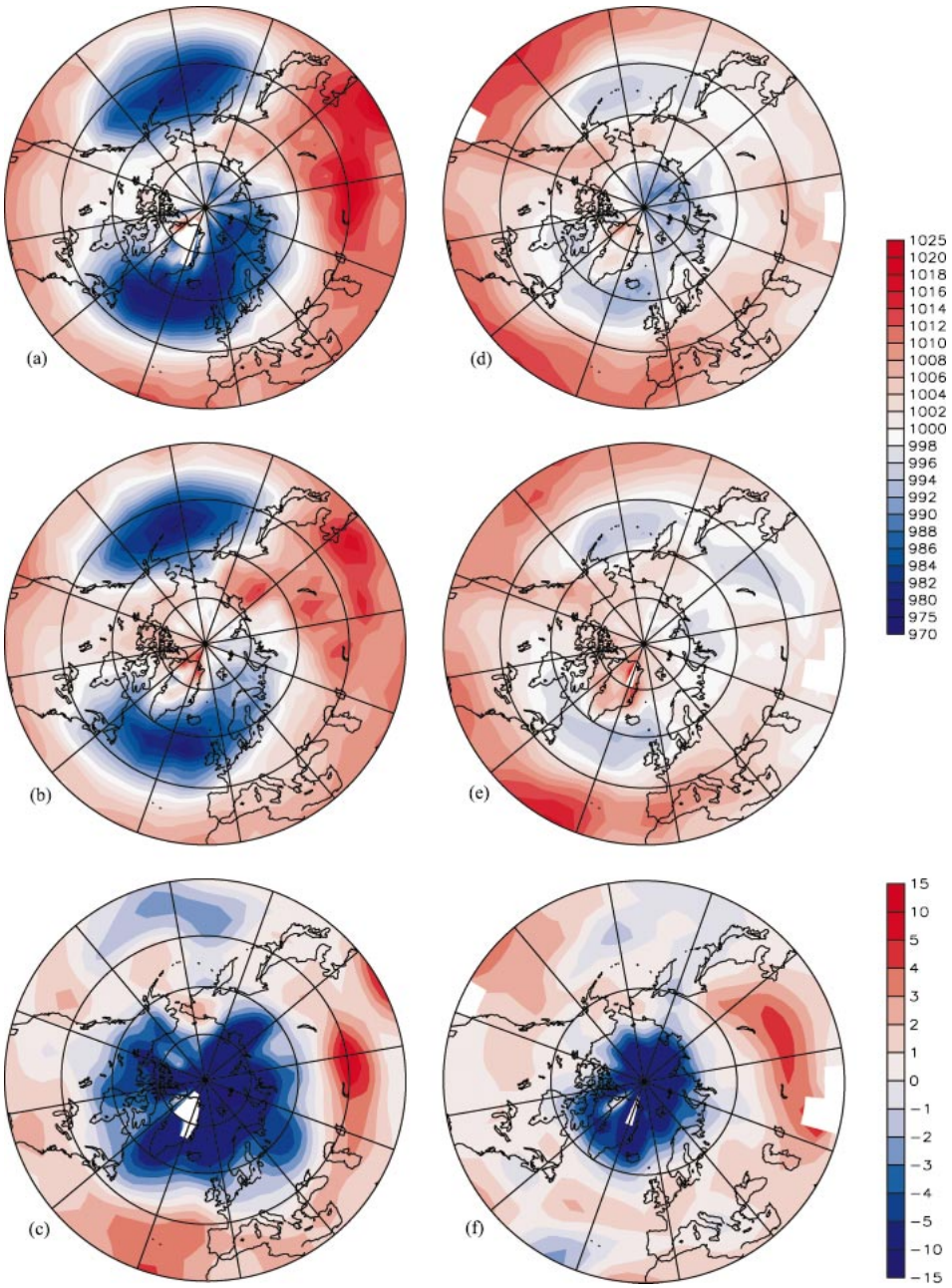

FIG. 14. The composite cyclone center SLP in the winters with the CAI anomalies (a) larger than 1.0 std dev, (b) less than −1.0 std dev, and (c) their difference. The composite cyclone center SLP in the summers with the CAI anomalies (d) larger than 1.0 std dev, (e) less than −1.0 std dev, and (f) their difference.

a broader domain in winter, from the Arctic Ocean to the subpolar regions in the North Atlantic, while the area of decrease contracts substantially in summer. Surrounding the SLP decrease, an area of SLP increase is apparent in the midlatitudes, with maxima in the North Atlantic and Eurasia in winter and in Eurasia and the northeast Pacific Ocean in summer. The pattern of SLP change between the negative and positive phase of the CAI displays the ''annular'' character of the AO mode.

7. Summary and conclusions

We analyzed the climatology and variability of the cyclone activity in the Arctic region and the northern midlatitudes during 1948–2002 using an automated algorithm of cyclone identification and tracking. The cyclone climatology is characterized by high cyclone center counts and low cyclone center SLP over the subpolar Pacific and Atlantic Oceans from the Sea of Okhotsk

TABLE 5. The years of the standard deviation of the CAI anomalies larger than 1.0 and less than −1.0.

	CAI anomaly larger than 1.0σ	CAI anomaly less than -1.0σ
Winters	1967/68, 1975/76, 1989/90, 1990/91, 1991/92, 1992/93, 1994/95	1951/52, 1952/53, 1958/59, 1960/61, 1965/66, 1966/67, 1968/69, 1969/70
Summers	1967, 1975, 1989, 1990, 1991, 1992, 1994	1951, 1952, 1958, 1960, 1965, 1966, 1968, 1969

to the Bering Sea and the Gulf of Alaska and from the southern Greenland Sea/the Iceland Sea to the Barents Sea. Our study reveals a strong seasonality that has not been explained heretofore. The Arctic cyclones are stronger in winter than summer, with larger seasonal amplitude in the marginal zone than the Arctic Ocean. The cyclone trajectory count is higher in summer and lower in winter and the cyclone duration is longer in summer than in winter. Therefore, there are fewer shorter and stronger cyclones in winter, and more numerous longer-lived, but weaker, cyclones in summer in the Arctic region. Moreover, the cyclones in the Arctic region can be generated both locally and in the midlatitudes. Our diagnosis indicates that the cyclones originating in the midlatitudes are stronger than those generated in the Arctic region.

Cyclone activity shows substantial interannual variability in the Arctic region, as portrayed by the newly defined integrative index, CAI. The CAI anomaly exhibits an apparent increasing trend over the study period. Superimposed on the long-term trend are large interannual fluctuations. In particular, the CAI anomaly was unprecedentedly amplified from 1988 to 1991, reflecting an intensification of the cyclone activity, which coincides with the sharp decrease of mean SLP over the Arctic Ocean (Walsh et al. 1996) and the increase of the AO index (Thompson and Wallace 1998). The increase in number and strength of cyclones from the midlatitudes, mainly from the North Atlantic and Eurasia, supports the persistence of the amplified cyclone activity during this period. Interaction of cyclone activity between the Arctic Ocean (70°–90°N) and the Arctic marginal zone (60°–70°N) plays a critical role in determining the Arctic cyclone activity in the entire Arctic region (60°–90°N). The synchronized variation of cyclone activity in the Arctic Ocean and the Arctic marginal zone amplifies the measures of cyclone activity in the entire Arctic region.

The CAI variability contains considerable power in several spectral bands. The major significant signals are characterized by low-frequency variation at a multidecadal time scale and oscillations at 7.8 and 4.1 yr. The low-frequency variation was in its low phase in the 1960s and high phase in the 1990s, corresponding well to the low-frequency variation of NAO (Dickson et al. 2000) and Arctic surface air temperature anomalies (Polyakov et al. 2002). Proshutinsky and Johnson (1997) proposed two regimes of the cyclonic and anticyclonic Arctic sea ice and ocean circulation, which are generally well correlated to the 7.8-yr oscillation in the cyclone activity. Such a relationship is useful in the diagnosis of large-scale atmosphere–sea ice–ocean interactions and in predictive application for sea ice and freshwater changes. Zhang et al.'s (2003) model study indicates that the high AO phase (generally high CAI anomalies) results in positive anomalies of sea ice and freshwater storage in the western Arctic Ocean and enhancement of sea ice and freshwater export via Fram Strait.

The cyclone activity in the Arctic region is significantly correlated with that in the midlatitudes. The cyclone activity in the midlatitudes shows an apparent decrease since the 1960s. The low-frequency variation of CAI anomalies in the North Atlantic and Eurasia is the opposite of that in the Arctic region. Negative correlation coefficients of cyclone trajectory and center counts between the Arctic and midlatitudes indicate a poleward shift of storm tracks. As reported by McCabe et al. (2001), cyclone center counts have increased in the Arctic region but decreased in the midlatitudes in recent decades, while the cyclone intensity increased in both the high- and midlatitudes. Our results show that the former conclusion extends to cyclone trajectories (individual cyclone events), and that the North Atlantic is the primary contributor to these variations. Moreover, our results indicate that the cyclone trajectory count variations may represent a low-frequency fluctuation or regime shift rather than a sustained linear trend. By analyzing NCEP–NCAR reanalysis data and output from climate modeling forced by greenhouse gas based on historical data and the Intergovernmental Panel on Climate Change IS92a scenario, Fyfe (2003) concluded that the number of cyclones has dramatically decreased in the Southern Hemisphere midlatitudes, while it has modestly increased over the Antarctic Ocean, suggesting a possible attribution to enhanced greenhouse gas concentrations. Given the linear increasing trend and the possible amplification of global warming, the poleward shift of the cyclone track in the Northern Hemisphere could also be a harbinger of climate change.

The composite fields of the cyclone center count and the cyclone center SLP, both of which are CAI components, bridge the synoptic and climate scales. They show seasonally varying differences between the two extremes of the CAI. The years of extreme positive (negative) phase mainly occurred after (before) 1970, showing an enhanced cyclone activity in the Arctic region. The major features corresponding to a transition from the negative to the positive phase are an increase of cyclone count in the Arctic region and a decrease in the subpolar band. The cyclone center SLP decreases in the Arctic region during the positive phase of CAI anomaly, while it increases in the midlatitudes, showing the ''annular'' characteristic of the AO mode. The area

of decreasing SLP shrinks in summer compared with winter.

Our results demonstrate that variations of Arctic cyclone activity are spatially and temporally complex. The cyclone variations will change the temporal characteristics of near-surface atmospheric parameters, which are directly relevant to sea ice deformation and upper-ocean currents. These are not well understood and are the focus of future research.

Acknowledgments. We thank the NOAA/CDC for making the NCEP–NCAR reanalysis data available. The ARSC supplied some computer resources. We thank M. Timlin for evaluating the temporal distribution of the most extreme events. We also thank Drs. S. Akasofu and R. Gerdes for their valuable comments. Finally, we are grateful to the editor, M. P. Hoerling, and two anonymous reviewers, whose careful and constructive reviews improved both presentation and content of this paper. Authors X. Zhang, U. S. Bhatt, and M. Ikeda were supported by the Japanese Marine Science and Technology Center through the International Arctic Research Center, University of Alaska, Fairbanks. J. E. Walsh was funded by the National Science Foundation through Grant OPP-0002239. J. Zhang was supported by funding from the University Partnership for Operational Support.

REFERENCES

Boer, G. J., 1995: Some dynamical consequences of greenhouse gas warming. *Atmos.–Ocean,* **33,** 731–751.

Clark, M. P., M. C. Serreze, and D. A. Robinson, 1999: Atmospheric controls on Eurasian snow extent. *Int. J. Climatol.,* **19,** 27–40.

Dickson, R. R., and Coauthors, 2000: The Arctic Ocean response to the North Atlantic Oscillation. *J. Climate,* **13,** 2671–2696.

Fyfe, J. C., 2003: Extratropic Southern Hemisphere cyclones: Harbingers of climate change? *J. Climate,* **16,** 2802–2805.

Ghil, M., and Coauthors, 2002: Advanced spectral methods for climatic time series. *Rev. Geophys.,* **40,** 1003, doi:10.1029/2000RG000092.

Graham, N. E., and H. F. Diaz, 2001: Evidence for intensification of North Pacific winter cyclones since 1948. *Bull. Amer. Meteor. Soc.,* **82,** 1869–1893.

Houghton, J. T., Y. Ding, D. G. Griggs, M. Noguer, P. J. van der Linden, X. Dai, K. Maskell, and C. A. Johnson, Eds., 2001: *Climate Change 2001: The Scientific Basis.* Cambridge University Press, 881 pp.

Kalnay, E., and Coauthors, 1996: The NCEP/NCAR 40-Year Reanalysis Project. *Bull. Amer. Meteor. Soc.,* **77,** 437–471.

Keegan, T. J., 1958: Arctic synoptic activity in winter. *J. Meteor.,* **15,** 513–521.

Kistler, R., and Coauthors, 2001: The NCEP–NCAR 50-Year Reanalysis: Monthly means CD-ROM and documentation. *Bull. Amer. Meteor. Soc.,* **82,** 247–268.

Lin, H., and J. Derome, 1998: A three-year lagged correlation between the North Atlantic Oscillation and winter condition over the North Pacific and North America. *Geophys. Res. Lett.,* **25,** 2829–2832.

Mann, M. E., and J. M. Lees, 1996: Robust estimation of background noise and signal detection in climatic time series. *Climatic Change,* **33,** 409–445.

McCabe, G. J., M. P. Clark, and M. Serreze, 2001: Trends in Northern Hemisphere surface cyclone frequency and intensity. *J. Climate,* **14,** 2763–2768.

Petterssen, S., 1950: Some aspects of the general circulation of the atmosphere. *Centenary Proc. of the Royal Meteorological Society,* London, United Kingdom, 120–153.

Polyakov, I., and Coauthors, 2002: Observationally based assessment of polar amplification of global warming. *Geophys. Res. Lett.,* **29,** 1878, doi:10.1029/2001GL011111.

Proshutinsky, A. Y., and M. A. Johnson, 1997: Two circulation regimes of the wind-driven Arctic Ocean. *J. Geophys. Res.,* **102,** 12 493–12 514.

Reed, R. J., and B. A. Kunkel, 1960: The Arctic circulation in summer. *J. Meteor.,* **17,** 489–506.

Rogers, J. C., 1990: Patterns of low-frequency monthly sea level pressure variability (1899–1986) and associated wave cyclone frequencies. *J. Climate,* **3,** 1364–1379.

Serreze, M. C., 1995: Climatological aspects of cyclone development and decay in the Arctic. *Atmos.–Ocean,* **33,** 1–23.

——, J. E. Box, R. G. Barry, and J. E. Walsh, 1993: Characteristics of Arctic synoptic activity, 1952–1989. *Meteor. Atmos. Phys.,* **51,** 147–164.

——, F. Carse, and R. Barry, 1997: Icelandic low cyclone activity: Climatological features, linkages with the NAO, and relationships with recent changes in the Northern Hemisphere circulation. *J. Climate,* **10,** 453–464.

——, A. H. Lynch, and M. P. Clark, 2001: The Arctic frontal zone as seen in the NCEP–NCAR reanalysis. *J. Climate,* **14,** 1550–1567.

Thompson, D. W., and J. M. Wallace, 1998: The Arctic Oscillation signature in the winter time geopotential height and temperature fields. *Geophys. Res. Lett.,* **25,** 1297–1300.

Trenberth, K. E., and J. W. Hurrell, 1994: Decadal atmosphere–ocean variations in the Pacific. *Climate Dyn.,* **9,** 303–319.

Walsh, J. E., W. L. Chapman, and T. L. Shy, 1996: Recent decrease of sea level pressure in the central Arctic. *J. Climate,* **9,** 480–486.

Whittaker, L. M., and L. H. Horn, 1982: Atlas of Northern Hemisphere extratropical cyclone activity, 1958–1977. University of Wisconsin—Madison, 65 pp.

Zhang, X., M. Ikeda, and J. E. Walsh, 2003: Arctic sea ice and freshwater changes driven by the atmospheric leading mode in a coupled sea ice–ocean model. *J. Climate,* **16,** 2159–2177.